PNAS Nexus, 2024, 3, 1–11
https://doi.org/10.1093/pnasnexus/pgae114
Advance access publication 12 March 2024
Research Report

Arginine with leucine drives reactive oxygen species-mediated integrin α5β1 expression and promotes implantation in mouse blastocysts

Momoka Nakazato[a,1], Mumuka Matsuzaki[a,1], Daiki Okai[a], Eisaku Takeuchi[a], Misato Seki[a], Miki Takeuchi[a], Emiko Fukui[a,b] and Hiromichi Matsumoto[a,b,*]

[a]Laboratory of Animal Breeding and Reproduction, Division of Animal Science, Department of Agrobiology and Bioresources, School of Agriculture, Utsunomiya University, Utsunomiya, Tochigi 321-8505, Japan
[b]Center for Bioscience Research and Education, Utsunomiya University, Utsunomiya, Tochigi 321-8505, Japan
*To whom correspondence should be addressed: Email: matsu@cc.utsunomiya-u.ac.jp
[1]M.N. and M.M. contributed equally to this work.
Edited By: Marisa Bartolomei

Abstract

The implantation rate of in vitro fertilization (IVF)-derived blastocysts after embryo transfer remains low, suggesting that the inadequate expression of specific proteins in culture-induced IVF-derived blastocysts contributes to low implantation rates. Therefore, treatment with appropriate regulation may improve the blastocyst implantation ability. This study demonstrated that the combination of L-arginine (Arg) and L-leucine (Leu) exerts distinct effects on IVF-derived mouse blastocysts. Arg with Leu promotes blastocyst implantation, whereas Arg alone decreases the blastocyst ability. Integrin α5β1 expression was increased in blastocysts treated with Arg and Leu. Arg with Leu also increased reactive oxygen species (ROS) levels and showed a positive correlation with integrin α5β1. Ascorbic acid, an antioxidant, decreased ROS and integrin α5β1 levels, which were elevated by Arg with Leu. Meanwhile, the mitochondrial membrane potential (ΔΨm) in blastocysts did not differ between treatments. Glutathione peroxidase (GPx) is involved in ROS scavenging using glutathione (GSH) as a reductant. Arg with Leu decreased GPx4 and GSH levels in blastocysts, and blastocysts with higher ROS levels had lower GPx4 and GSH levels. In contrast, Arg alone increased the percentage of caspase-positive cells, indicating that Arg alone, which attenuated implantation ability, was associated with apoptosis. This study revealed that elevated ROS levels induced by Arg with Leu stimulated integrin α5β1 expression, thereby enhancing implantation capacity. Our results also suggest that ROS were not due to increased production by oxidative phosphorylation, but rather to a reduction in ROS degradation due to diminished GPx4 and GSH levels.

Keywords: blastocyst, implantation, reactive oxygen species

Significance Statement

Embryo transfer of blastocysts derived from in vitro fertilization (IVF) results in a low implantation rate, suggesting poor blastocyst quality for successful implantation and pregnancy. Amino acids have been shown to improve in vitro development of preimplantation embryos. In this study, we demonstrated that the combination of Arg and Leu exerted distinct effects on blastocyst implantation ability. Arg with Leu promotes blastocyst implantation. In particular, elevated reactive oxygen species (ROS) levels induced by Arg with Leu stimulate integrin α5β1 expression, thereby enhancing implantation capacity. This ROS was not due to increased production by oxidative phosphorylation but rather to a reduction in ROS degradation due to diminished glutathione peroxidase 4 and scavenging using glutathione levels.

Introduction

In vitro fertilization (IVF) and embryo transfer (ET) are technologies commonly used in reproductive biology, including assisted reproductive technology (ART) in humans. Despite the transfer of high-quality blastocysts, the implantation rate of IVF-derived blastocysts after ET remains low (1–4), with poor blastocyst implantation potential being one of the limiting factors for low pregnancy success in IVF. The inadequate expression of specific proteins in culture-induced IVF-derived blastocysts contributes to low implantation rates (5–7). We previously reported that proper treatment to induce proper regulation in in vitro culture before ET improves implantation rates and postimplantation embryonic development (6).

Competing Interest: The authors declare no competing interest.
Received: November 16, 2023. **Accepted:** March 5, 2024

Implantation of blastocysts into the maternal uterus is a crucial step in mammalian reproduction (7, 8). For successful implantation, the blastocyst must attain implantation competency in the receptive uterus (7–10). Highly coordinated cellular and molecular events produce a receptive uterine environment that supports implantation (7–11). Blastocysts also function as an active unit in this process, with their own molecular program of cell growth and differentiation (7, 8).

Trophoblast outgrowth is a reliable marker for trophoblast differentiation and migration (12, 13). L-arginine (Arg) and L-leucine (Leu) are necessary and sufficient for inducing trophoblast motility during outgrowth in vitro (14). Arg is essential during pregnancy for conceptus growth and development as a precursor for the synthesis of molecules (e.g. nitric oxide [NO], polyamines, and creatine) with cell signaling and metabolic functions (15). Arg is metabolized by NO synthase (NOS) to NO (16). NOS has been identified as three isoforms: type I or neuronal NOS (nNOS), type II or inducible form (iNOS), and type III or endothelial form (eNOS) (17). Our recent results showed that both iNOS and phosphorylated eNOS were expressed in implantation-induced blastocysts in vivo (18). Therefore, Arg and Leu may act during the induction of blastocyst implantation competence.

In the present study, we investigated whether Arg and Leu regulate the implantation ability of IVF-derived mouse blastocysts. In addition to the implantation rate, we examined the integrin α5β1 expression. Furthermore, we examined the levels of O_2, NO, reactive oxygen species (ROS), $\Delta\Psi_m$, glutathione peroxidase 1 (GPx1), GPx4, and scavenging using glutathione (GSH) in blastocysts by treatment of Arg with or without Leu. Our results showed that Arg with Leu upregulated implantation rate and ROS-dependent integrin α5β1. We also found that GPx4 and GSH levels were suppressed by Arg with Leu in blastocysts having high ROS levels.

Results

Arg with Leu promotes blastocyst implantation while Arg alone decreased the ability of blastocysts

To examine the embryonic potential of the transferred blastocysts during the peri-implantation period, untreated or treated blastocysts were transferred to the same pseudopregnant recipient, i.e. six untreated blastocysts (control) and six treated blastocysts (Arg and/or Leu) were transferred into distinct uterine horns in each recipient (Fig. 1A). The implantation rate of blastocysts treated with Arg and Leu (mean ± SEM) was significantly higher than that of the control (83.3 ± 5.8 vs. 61.1 ± 7.5%; $P < 0.05$; Fig. 1A and B). Meanwhile, treatment with Arg alone decreased blastocyst implantation rate as compared to control (53.1 ± 7.4 vs. 77.3 ± 5.6%; $P < 0.05$; Fig. 1B). The implantation rates of blastocysts treated with Leu alone (78.8 ± 8.1%) was not significantly different from that of the control (71.2 ± 8.1%; $P > 0.05$; Fig. 1B).

Integrin signaling is a key function in trophoblast-uterine communication during implantation, especially integrin α5β1 expression and translocation are involved in adhesion competence during the preimplantation period in blastocysts (19, 20). To examine the ability of blastocysts before transfer, we analyzed the expression of integrin α5β1 (Fig. 1C and S1). Integrin α5β1 expression was significantly increased in the blastocysts by Arg with Leu (1.74 ± 0.14; $P < 0.05$), but not by Arg (1.22 ± 0.09) or Leu (0.99 ± 0.09), as compared to the control (1.00 ± 0.09) ($P > 0.05$; Fig. 1C and D). These findings indicate that Arg with Leu upregulates integrin α5β1 and enhances the implantation ability of blastocysts.

Decreased O_2 consumption by Arg with Leu or Arg alone is NO-independent

Arg is metabolized by NOS to NO (16). Moreover, Arg affects blastocyst oxygen (O_2) consumption, possibly by enhancing NO production (21). To determine the effect of Arg with or without Leu, we simultaneously analyzed NO production and O_2 consumption in individual blastocysts (Figs. 2A and S2). NO production was significantly increased in blastocysts treated with Arg (1.17 ± 0.05; $P < 0.05$), but not by Arg with Leu (0.93 ± 0.04; $P > 0.05$), as compared to the control (1.00 ± 0.05; Fig. 2A and B).

O_2 consumption was significantly decreased in the blastocysts by Arg with Leu (0.30 ± 0.01), and Arg (0.40 ± 0.02) as compared to control (1.00 ± 0.05; $P < 0.05$; Fig. 2A and C). O_2 consumption in blastocysts treated with Arg and Leu was significantly lower than in blastocysts treated with Arg alone ($P < 0.05$; Fig. 2C).

The relationship between NO production and O_2 consumption was determined using the Pearson correlation coefficient and linear regression analysis (Fig. 2D–F). Neither Arg with Leu nor Arg alone indicated significant correlations between NO production and O_2 consumption ($P > 0.05$; Fig. 2E and F), whereas control blastocysts showed a significant correlation ($P < 0.05$; Fig. 2D). These findings indicated that decreased O_2 consumption by Arg with Leu or Arg alone is NO-independent, whereas Arg alone increases NO production.

ROS increases with unaltered mitochondrial activity in blastocysts by treatment of Arg with Leu or Arg alone

Oxygen consumption in blastocysts reflects mitochondrial function and dysfunction, whereas ROS normally arise as by-products of the mitochondrial electron transport chain (22). Mitochondrial membrane potential is a key indicator of mitochondrial activity because it reflects the processes of electron transport and oxidative phosphorylation (23). To determine the effects of Arg with or without Leu, JC-1 staining and ROS assays were performed in individual blastocysts (Figs. 3A and S3). Mitochondrial membrane potential ($\Delta\Psi_m$) was evaluated by JC-1 staining using the ratio of red (aggregate, high $\Delta\Psi$) and green (monomeric, low $\Delta\Psi$) fluorescence. Pink areas show colocalization of red (high $\Delta\Psi$) and blue (ROS), i.e. ROS production in the active mitochondria.

$\Delta\Psi_m$ in blastocysts were not different in any treatment of control (1.00 ± 0.08), Arg with Leu (0.89 ± 0.06), and Arg (0.94 ± 0.07; $P > 0.05$; Fig. 3B). Meanwhile, ROS level was significantly increased in blastocysts treated with Arg and Leu (2.22 ± 0.13), and Arg alone (1.68 ± 0.10) compared to control (1.00 ± 0.06; $P < 0.05$; Fig. 3A and C). ROS levels in blastocysts treated with Arg and Leu were significantly higher than those in blastocysts treated with Arg alone ($P < 0.05$; Fig. 3C).

The relationship between $\Delta\Psi_m$ and ROS level was determined (Fig. 3D–F). Arg with Leu showed a significant correlation between $\Delta\Psi_m$ and ROS ($P < 0.05$; Fig. 3E), while neither control nor Arg alone showed a significant correlation ($P > 0.05$; Fig. 3D and F). These findings indicate that increased ROS levels by Arg with Leu are derived from active mitochondria, while the mitochondrial membrane potential is unaltered.

Integrin α5β1 is downstream of ROS increased by Arg with Leu

As shown in Fig. 1, Arg and Leu, which enhance implantation ability, induced integrin α5β1 expression. Furthermore, an increase in ROS levels was induced by Arg and Leu (Fig. 3). ROS play a role in both outside-in and inside-out integrin signaling, raising the

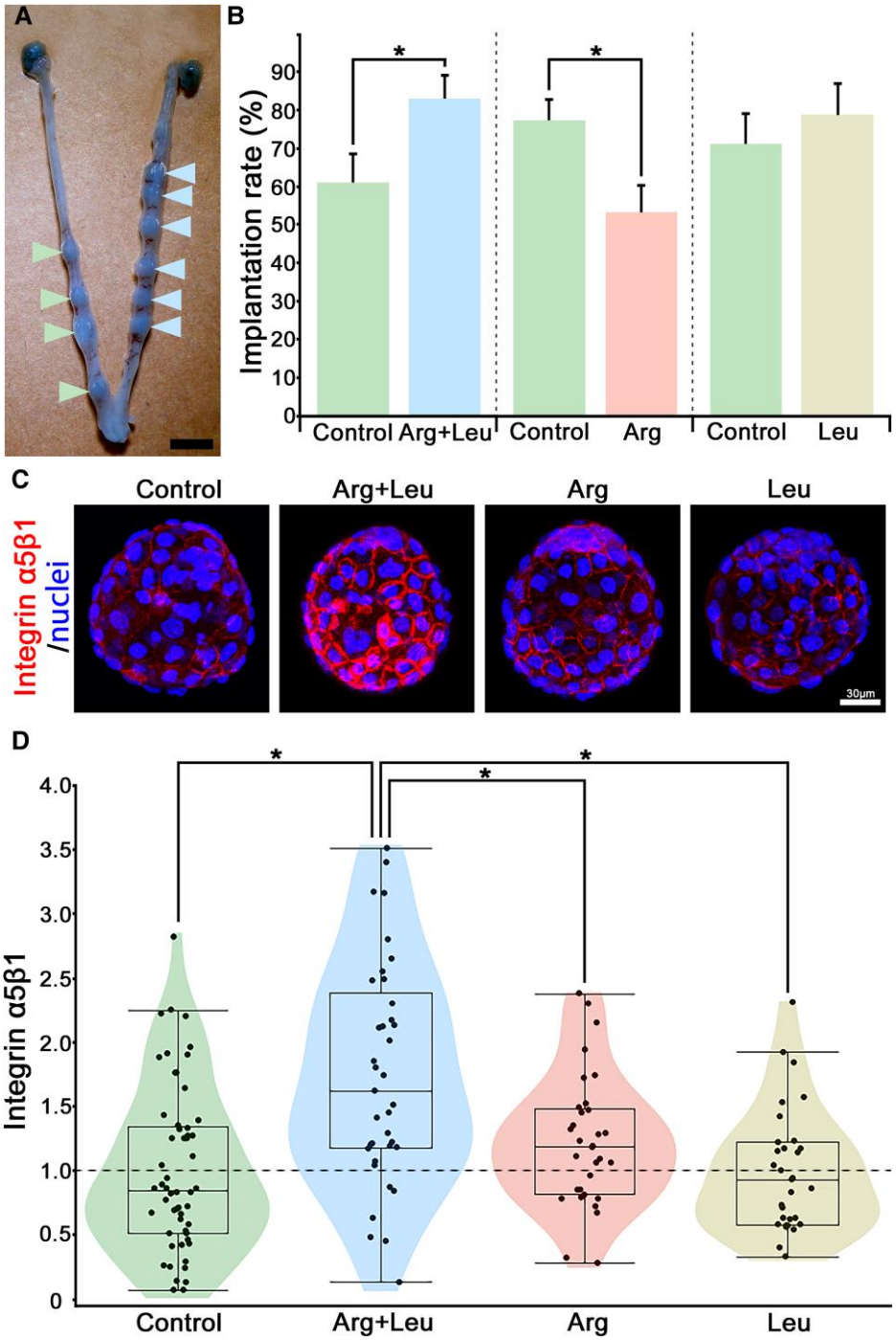

Fig. 1. Diverse effects of Arg and/or Leu on the implantation ability of IVF-derived mouse blastocysts. A) Six untreated blastocysts (control) or six blastocysts treated with Arg + Leu were transferred to one (left) or the other uterine horn (right) of the same pseudopregnant recipient. Green and blue arrowheads indicate the implantation sites of untreated (control) embryos and those treated with Arg + Leu, respectively. (Scale bar, 5 mm.) B) Implantation rates after ET of blastocysts treated with Arg + Leu, Arg, or Leu. Data are presented as mean ± SEM. Statistical significance was determined using Student's *t* test; *$P < 0.05$. The sample sizes of recipient females for treatment with Arg + Leu, Arg, or Leu were $n = 12$, 11, or 11, respectively. C) Immunostaining showing increased expression of integrin α5β1 (red) in the TE of blastocysts treated with Arg + Leu. The nuclei were stained blue with Hoechst 33342 (Scale bar, 30 μm). D) Scatter-box-violin plots displaying integrin α5β1 level. Integrin α5β1 expression levels were evaluated as relative values, with the average fluorescence intensities of the control as 1. Violin plots displaying the probability density of data. $n = 56$, 37, 32, and 31 for treatments of control, Arg + Leu, Arg, and Leu, respectively. Statistical significance was determined using the Steel–Dwass test; *$P < 0.05$.

possibility that ROS constitute master regulators of crosstalk between these fundamental cell adhesion receptors (24, 25). Therefore, to clarify the relationship between ROS and integrin α5β1, blastocysts were treated with antioxidants using ascorbic acid and analyzed individually.

ROS levels, which were elevated in Arg and Leu (1.53 ± 0.07) compared to the Control (1.00 ± 0.05), were decreased by ascorbic acid treatment (1.10 ± 0.05; $P < 0.05$; Figs. 4A and S4). Integrin α5β1 expression showed a similar transition, i.e. integrin α5β1 level, which was elevated in Arg and Leu (2.52 ± 0.18) compared to the

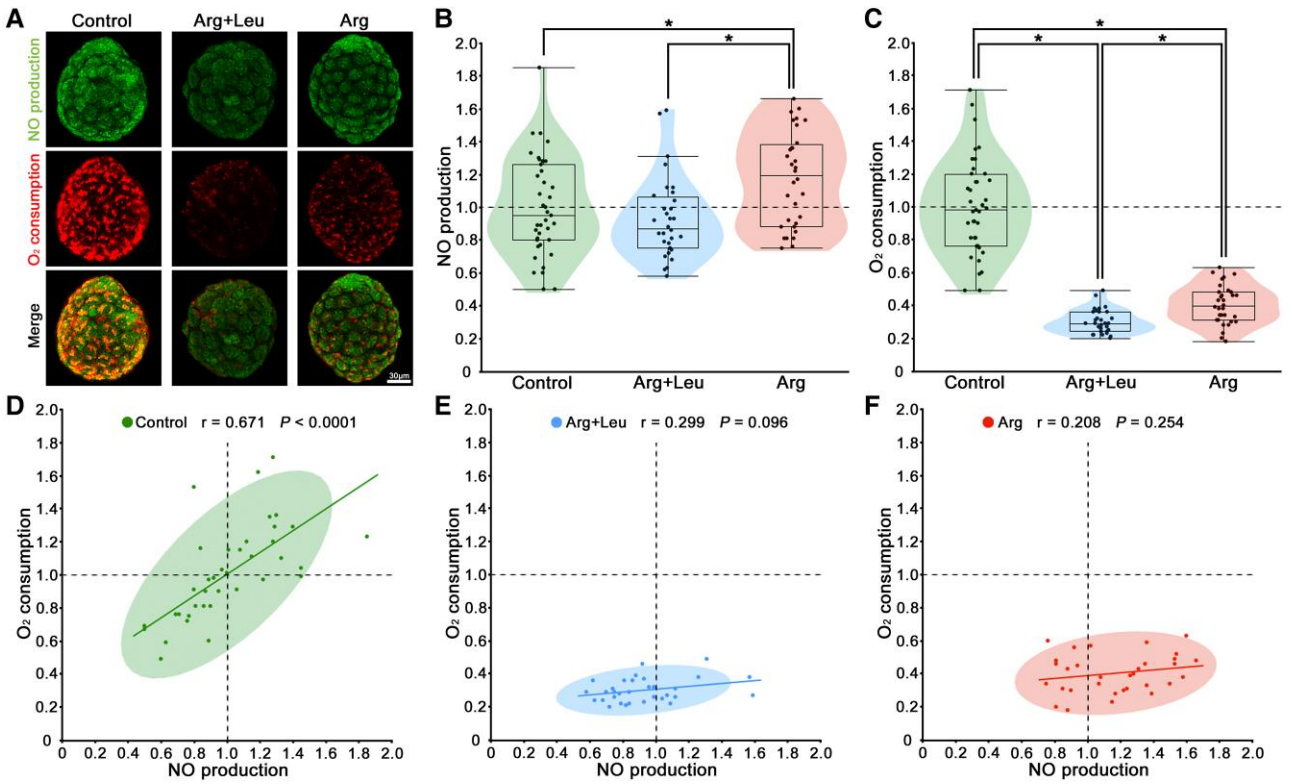

Fig. 2. NO production and O_2 consumption in individual blastocysts by treatment of Arg with Leu or Arg alone. A) Distribution of NO production (green) and O_2 consumption (red) (Scale bar, 30 μm). B and C) Scatter-box-violin plots displaying NO production (B) and O_2 consumption (C). NO production and O_2 consumption were evaluated as relative values, with the average fluorescence intensity of the control being 1. Violin plots displaying probability density of data. $n = 39$, 32, and 32 for the control, Arg + Leu, and Arg treatments, respectively. Statistical significance was determined using Steel–Dwass test; $^*P < 0.05$. D–F) Scatterplots displaying the correlation between NO production and O_2 consumption in individual blastocysts for control (D), Arg + Leu (E), or Arg (F) treatments. The ellipses represent 90% CIs.

control (1.00 ± 0.11), was decreased in ascorbic acid treatment (1.15 ± 0.16; $P < 0.05$; Figs. 4B and S4). The relationship between ROS and integrin α5β1 levels was determined (Fig. 4C–E). Control blastocysts showed a significant negative correlation ($P < 0.05$; Fig. 4C). Meanwhile, Arg with Leu (Fig. 4D) and Arg with Leu plus ascorbic acid (Fig. 4E) showed significant positive correlations ($P < 0.05$). Moreover, Fisher's exact probability test indicated that the percentage of blastocysts with both ROS and integrin α5β1 levels in the range above 1.00 was decreased significantly by ascorbic acid (35.5%, 11/31; $P < 0.05$) compared to Arg and Leu (88.6%, 31/35; Fig. 4D and E). These findings indicate that ROS is upstream of integrin α5β1.

Total number of cells in blastocysts was not different in any treatment of control (93.1 ± 2.1), Arg with Leu (93.4 ± 2.0), and ascorbic acid treatment for Arg with Leu (88.8 ± 2.1; $P > 0.05$; Fig. S5). Correlation analysis between the total number of cells and ROS showed significant positive correlations in the control and Arg with Leu ($P < 0.05$; Fig. S6A and B), but not in Arg with Leu plus ascorbic acid treatment ($P > 0.05$; Fig. S6C). Meanwhile, integrin α5β1 expression did not correlate with the total number of cells in any of the treatments (Fig. S7A–C). These findings indicate that ROS levels in blastocysts depend on the number of cells, while integrin α5β1 is independent of cell number.

GPx4 is downregulated by Arg with Leu

As shown in Fig. 3, increased ROS levels induced by Arg with Leu or Arg alone are derived from active mitochondria, while the mitochondrial membrane potential is unaltered. Therefore, we hypothesized that elevated ROS levels were the result of accumulation rather than increased ROS production. Glutathione peroxidases (GPxs) are key enzymes involved in scavenging reactive ROS using GSH as a reductant (26, 27). To determine the source of ROS, we examined the distribution of GPx1, GPx4, GSH, and ROS in individual blastocysts (Figs. 5 and S8).

GPx1 was expressed in both the cytoplasm and nuclei with all treatments, and GPx1 levels were not different in any treatment of control (1.00 ± 0.11), Arg with Leu (0.96 ± 0.12), and Arg alone (1.17 ± 0.12; $P > 0.05$; Fig. 5A). The relationship between GPx1 and ROS levels was determined (Fig. 5D–F). Neither control nor Arg with Leu showed significant correlations ($P > 0.05$; Figs. 5D and E), while Arg alone showed a significant correlation between GPx1 and ROS ($P < 0.05$; Fig. 5F).

Meanwhile, GPx4 level was significantly decreased in the blastocysts by Arg with Leu (0.81 ± 0.03; $P < 0.05$) as compared to control (1.00 ± 0.04) and Arg alone (0.98 ± 0.06) (Fig. 5B). GPx4 expression was reduced but remained in the nuclei by Arg with Leu, whereas GPx4 was expressed in both the cytoplasm and nuclei in the control and Arg alone (Fig. 5B). The relationship between GPx4 and ROS levels was determined (Fig. 5G–I). Arg with Leu and Arg alone showed significant correlations between GPx4 and ROS ($P < 0.05$; Fig. 5H and I), while the control did not show a significant correlation ($P > 0.05$; Fig. 5G). In particular, in the Arg with Leu treatments, which showed a significant correlation, all (100%, 30/30) blastocysts had ROS levels above 1.00, whereas 83.3% (25/30) of blastocysts had GPx4 levels below 1.00 (Fig. 5H).

Correlation analysis between GPx1 and GPx4 showed that the control group did not show significant correlations ($P > 0.05$; Fig. S9A), while Arg with Leu and Arg alone showed a significant

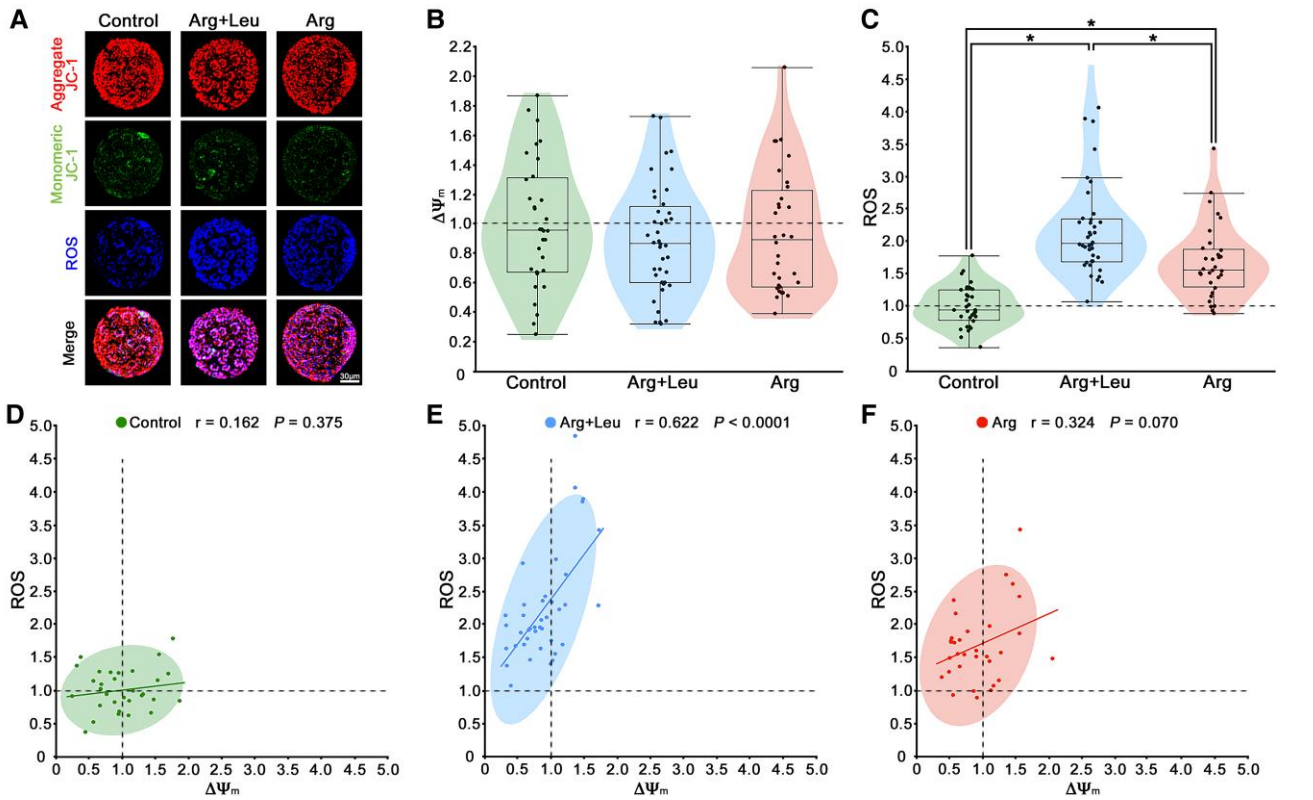

Fig. 3. Mitochondrial membrane potential ($\Delta\Psi_m$) and ROS levels in individual blastocysts after treatment of Arg with Leu or Arg alone. (A) Distribution of aggregate JC-1 (red, high $\Delta\Psi$), monomeric JC-1 (green, low $\Delta\Psi$), and ROS levels (blue). Overlay of high $\Delta\Psi$ (red) and ROS (blue) with colocalization appears as pink regions in the blastocysts (Scale bar, 30 μm). B and C) Scatter-box-violin plots displaying $\Delta\Psi_m$ (the ratio of red to green) (B) and ROS levels (C). The $\Delta\Psi_m$ and ROS levels were evaluated as relative values, with the average fluorescence intensity of the control being 1. Violin plots displaying probability density of data. $n = 32$, 40, and 32 for the control, Arg + Leu, and Arg treatments, respectively. Statistical significance was determined using Steel–Dwass test; *$P < 0.05$. D–F) Scatterplots displaying the correlation between $\Delta\Psi_m$ and ROS levels in individual blastocysts treated with control (D), Arg + Leu (E), or Arg (F). The ellipses represent 90% CIs.

correlation ($P < 0.05$; Fig. S9B and C). In the Arg with Leu treatments, 83.3% (25/30) of the blastocysts had GPx4 levels in the range below 1.00, while 56.7% (17/30) of the blastocysts had GPx1 levels below 1.00 (Fig. S9B). These findings indicate that the high levels of ROS induced by Arg with Leu are mainly derived from accumulation due to GPx4 reduction.

GSH level is decreased by Arg with Leu

Glutathione is present in either the reduced (GSH) or oxidized glutathione (GSSG) form, and GSH acts as a strong reducing agent and serves as an electron donor for GPxs (28). Therefore, GSH, as a reductant that scavenges ROS, should be localized with GPxs. Indeed, GSH was localized in the nuclei in all treatments (Fig. 5C) as well as GPx4 (Fig. 5B), but was distributed differently from GPx1 (Fig. 5A). Furthermore, GSH levels showed a similar transition as GPx4, i.e. GSH level was significantly decreased in blastocysts by Arg with Leu (0.68 ± 0.02) as compared to the control (1.00 ± 0.04) and Arg alone (0.92 ± 0.03; $P < 0.05$; Fig. 5C). The relationship between GSH and ROS levels was determined (Fig. 5J–L). There was a significant correlation between GSH and ROS in Arg with Leu and Arg alone ($P < 0.05$; Fig. 5K and L) but not in the control ($P > 0.05$; Fig. 5J). In particular, in the Arg with Leu treatments, all blastocysts (100%, 30/30) had ROS levels in the range above 1.00, whereas all blastocysts (100%, 30/30) had GSH levels below 1.00 (Fig. 5K).

Correlation analysis between GSH and GPx1 showed that the control did not indicate significant correlations ($P > 0.05$; Fig. S10A), while Arg with Leu and Arg alone indicated significant correlations ($P < 0.05$; Fig. S10B and C). Meanwhile, all treatments showed a significant correlation between GSH and GPx4 ($P < 0.05$; Fig. S11A–C). The percentage of blastocysts with both GPx4 and GSH levels in the range below 1.00 significantly increased by Arg with Leu (83.3%, 25/30; Fig. S11B) than in the control (46.7%, 14/30; Fig. S11A) and Arg alone (46.7%, 14/30; Fig. S11C) ($P < 0.05$). These findings indicate that high levels of ROS by Arg with Leu, in addition to lower GPx4 levels, are also derived from accumulation due to GSH supply shortage.

Apoptosis is upregulated by Arg alone

As shown in Fig. 2B, the NO level was significantly increased in blastocysts treated with Arg alone as compared to the control and Arg with Leu. Excessive NO leads to apoptosis in embryos and has deleterious effects on embryonic development (29–31). Therefore, apoptosis may be associated with an Arg-induced increase in the NO levels. To address this issue, active caspases were evaluated in individual blastocysts (Figs. 6A and S12). Percentage of caspase-positive cells was increased in Arg alone ($6.1 \pm 0.5\%$) compared to Arg with Leu ($4.3 \pm 0.4\%$; $P < 0.05$), but not different in Control ($5.4 \pm 0.5\%$; $P > 0.05$) (Fig. 6A and B). Meanwhile, total number of cells were not different in any treatment of control (82.4 ± 1.9), Arg with Leu (83.5 ± 1.8), and Arg alone (81.4 ± 1.7; $P > 0.05$; Fig. 6C). The relationship between the total number of cells and the percentage of caspase-positive cells was determined (Fig. 6D–F). All treatments showed a significant

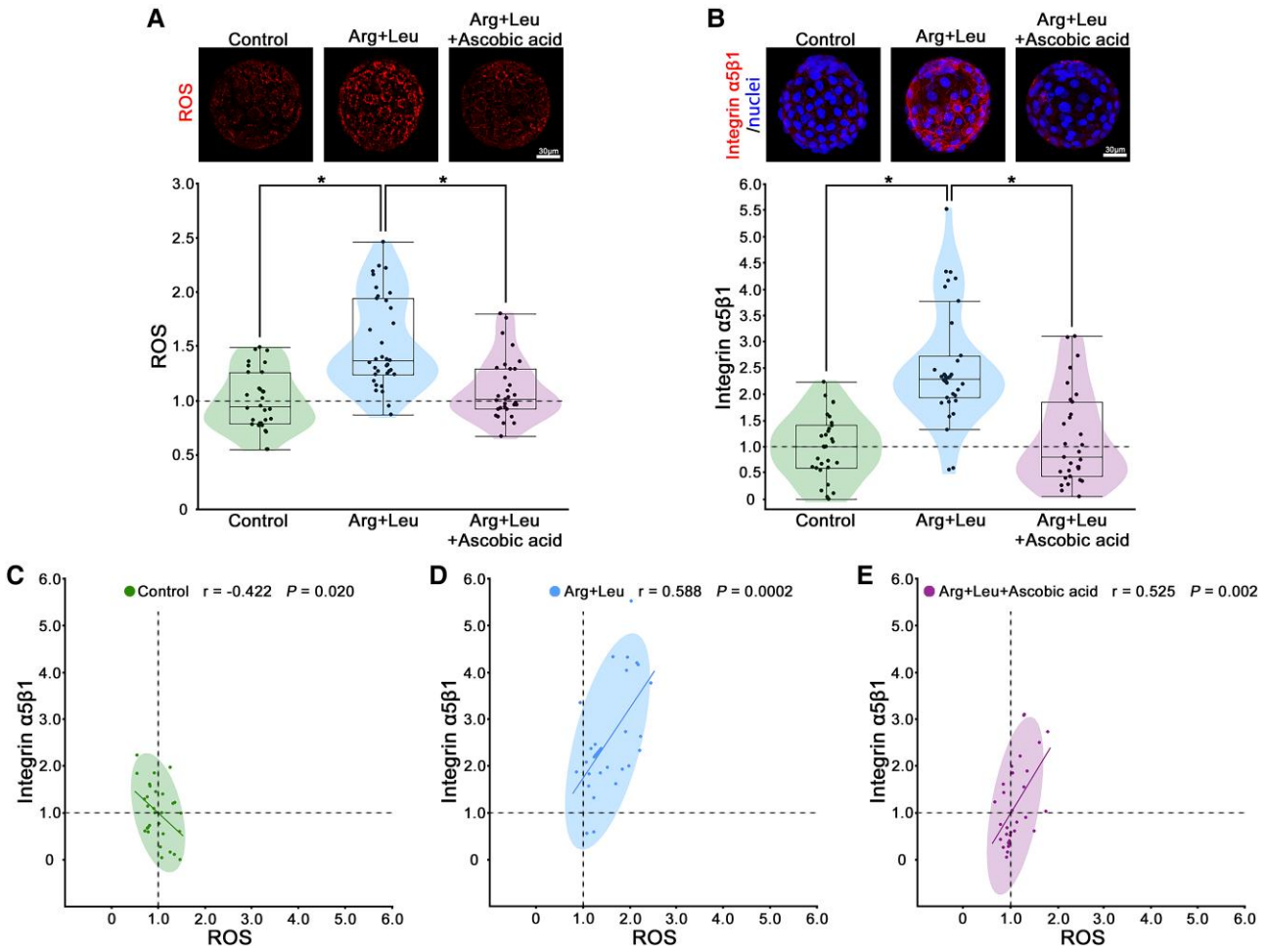

Fig. 4. ROS increased by Arg with Leu is upstream of integrin α5β1. A and B) Detection and scatter-box-violin plots displaying ROS (A) and integrin α5β1 (B) in blastocysts treated with antioxidant, ascorbic acid. ROS and integrin α5β1 levels were evaluated as relative values, with the average fluorescence intensity of the control being 1. Violin plots displaying probability density of data. $n = 30$, 35, and 31 for the control, Arg + Leu, and Arg + Leu + ascorbic acid, respectively. Statistical significance was determined using Steel–Dwass test; *$P < 0.05$. C–E) Scatterplots displaying the correlation between ROS and integrin α5β1 in individual blastocysts for the control (C), Arg + Leu (D), or Arg + Leu + ascorbic acid (E). The ellipses represent 90% CIs.

negative correlation between the total number of cells and the percentage of caspase-positive cells ($P < 0.05$; Fig. 6D–F). These findings indicate that Arg alone, which attenuates implantation ability, is associated with apoptosis in part but does not affect cell proliferation.

Discussion

Amino acids have been shown to improve in vitro development of preimplantation embryos (32–34). In this study, we demonstrated that the combination of Arg and Leu exerts distinct effects on blastocyst implantation ability. In particular, elevated ROS levels induced by Arg with Leu stimulated integrin α5β1 expression, thereby enhancing implantation capacity. This ROS was not due to increased production by oxidative phosphorylation but rather to a reduction in ROS degradation due to diminished GPx4 and GSH levels.

Blastocyst implantation involves three processes: apposition, attachment, and invasion of blastocysts (35, 36). Trophoblast motility begins after the onset of attachment. An in vitro trophoblast outgrowth assay showed that 0.2 mM Arg and 0.2 mM Leu act individually and additively to propagate signals that induce trophoblast motility (14). In vitro culture also showed that blastocysts exhibit increased integrin trafficking to the plasma membrane and subsequently acquire the ability to become adhesive, as demonstrated by their binding to fibronectin beads (37–40). These changes in integrin distribution and fibronectin binding occur even in the absence of an amino acid signal (41). In the present study, we showed that a simple combination of potassium simplex optimized medium (KSOM) culture medium and amino acids can modulate the implantation ability of blastocysts, i.e. when blastocysts were transferred into the uteri on the morning of the 4th day of pregnancy and implantation was assessed two days later, an increase in the implantation rate was observed with the combination of Arg and Leu. In contrast, the implantation rate decreased with Arg alone, whereas no significant change was observed with Leu alone. We also found that Arg with Leu upregulated integrin α5β1, but not Arg or Leu alone. These results suggest that upregulation of integrin α5β1 by Arg with Leu in vitro is the key to enhancing the attachment ability of blastocysts during implantation.

The present study revealed that elevated ROS levels in blastocysts induced by Arg with Leu were associated with integrin α5β1 protein expression. Integrins and their extracellular matrix (ECM) ligands are targets of ROS, which can influence integrin-mediated signaling by inducing the conformational changes required for integrin activation (24, 42–44). Thus, ROS can function

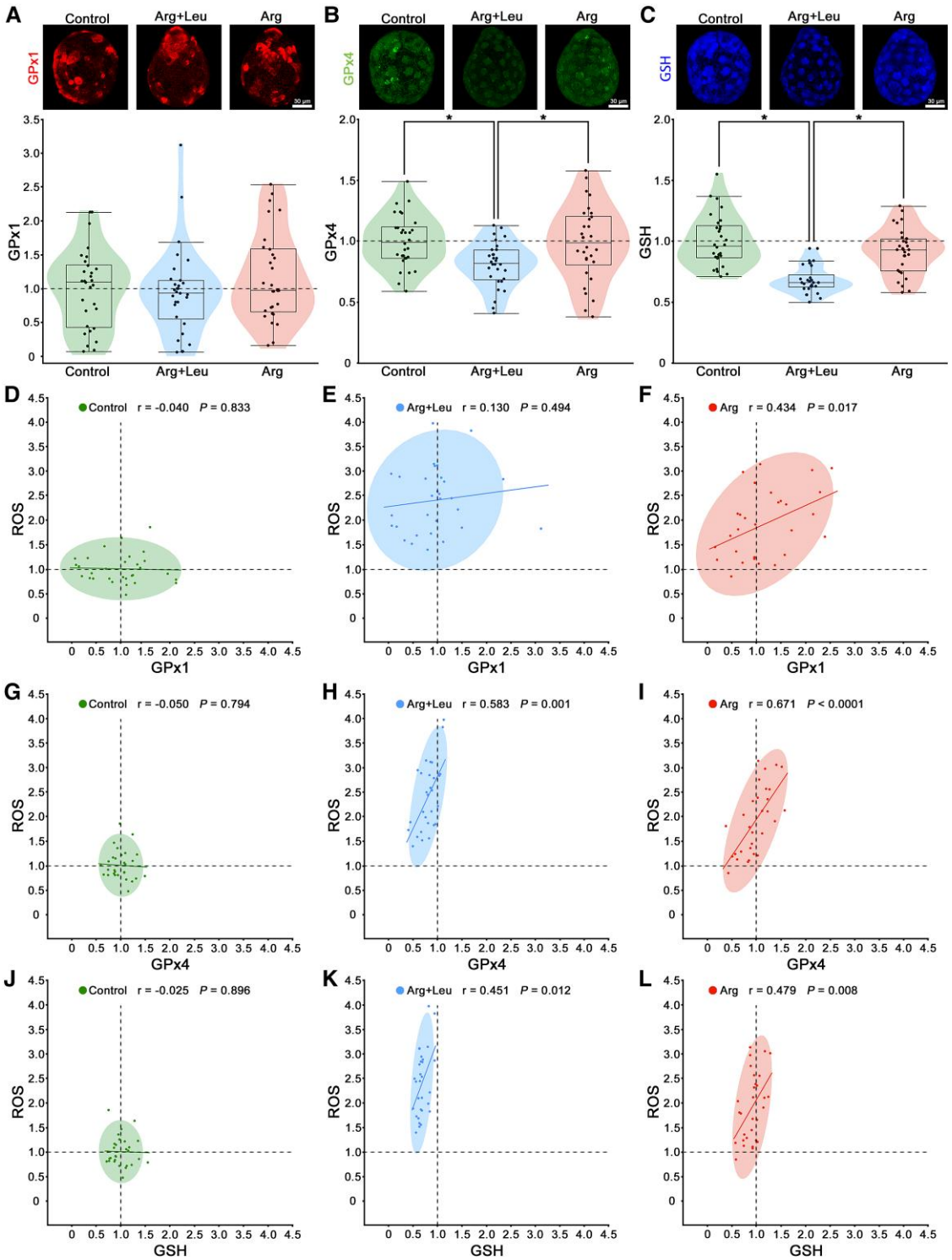

Fig. 5. Distribution of GPx1, GPx4, and GSH in individual blastocysts after treatment of Arg with Leu or Arg alone. A–C) Detection and scatter-box-violin plots displaying GPx1 (A), GPx4 (B), and GSH (C). GPx1, GPx4, and GSH levels were evaluated as relative values, with the average fluorescence intensity of the control being 1. Violin plots displaying probability density of the data. $n = 30$, 30, and 30 for the control, Arg + Leu, and Arg treatments, respectively. Statistical significance was determined using Steel–Dwass test; $^*P < 0.05$. D–F) Scatterplots displaying the correlation between GPx1 and ROS in individual blastocysts treated with control (D), Arg + Leu (E), or Arg (F). G–I) Scatterplots displaying the correlation between GPx4 and ROS in individual blastocysts treated with control (G), Arg + Leu (*H*) or Arg (*I*). (*J*–*L*) Scatterplots displaying the correlation between GSH and ROS in individual blastocysts treated with control (J), Arg + Leu (K), or Arg (L). The ellipses represent 90% CIs.

as important signaling molecules and key regulators of gene expression (45). However, our results indicate that ROS function to improve blastocyst implantation ability is mainly a translational response, including integrin α5β1. Generally, high ROS levels are detrimental to the development of embryos in culture, and the administration of free radical scavengers improves embryo development in vitro (46–48). Arg with Leu showed significant positive correlations with ROS and integrin α5β1 levels. Meanwhile,

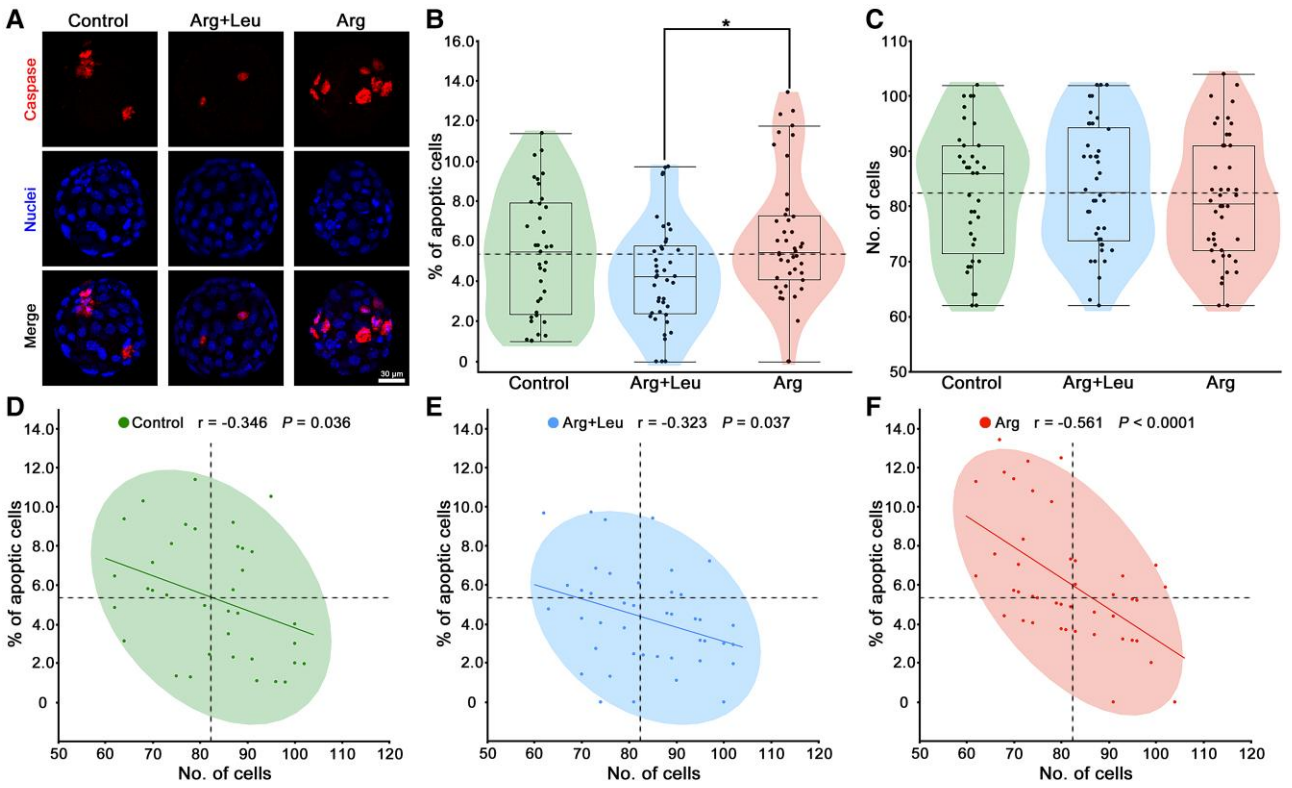

Fig. 6. Detection of active caspases in individual blastocysts after treatment of Arg with Leu or Arg alone. A) Distribution of active caspases (red) and nuclei (blue) (Scale bar, 30 μm). B and C) Scatter-box-violin plots displaying the percentage of caspase-positive cells (B) and total number of cells (C). Violin plots displaying probability density of data. $n = 37$, 42, and 44 for treatments with control, Arg + Leu, and Arg, respectively. Statistical significance was determined using Steel–Dwass test; $^*P < 0.05$. D–F) Scatterplots displaying the correlation between the total number of cells and the percentage of caspase-positive cells in individual blastocysts treated with control (D), Arg + Leu (E), or Arg (F). The ellipses represent 90% CIs.

blastocysts cultured in KSOM (control) showed significant negative correlations between ROS and integrin α5β1 levels, indicating that blastocysts with higher ROS levels possessed lower integrin α5β1 expression. This is similar to the well-known results of preimplantation embryo culture that higher ROS levels are detrimental to embryonic development and suggests that KSOM without Arg or Leu, which is commonly used for mouse embryo culture, is insufficient for blastocyst implantation. Therefore, our results also suggest that Arg with Leu leads to changes in the physiological fate of blastocysts, i.e. from the preimplantation to the attachment phase. Furthermore, the transition to implanting blastocysts possesses different physiological mechanisms and nutritional requirements than the development of blastocysts, suggesting the important role of amino acids such as Arg and Leu.

In a biological context, ROS are formed as a natural by-product of cellular aerobic metabolism, and mitochondrial respiration is a significant cause of ROS (49, 50). Our results showed that elevated ROS levels were induced by Arg with Leu, whereas mitochondrial membrane potential was unaltered by Arg with Leu. Furthermore, O_2 consumption was decreased by Arg with Leu. These results indicate that the elevated ROS levels induced by Arg with Leu were not derived from increased cellular aerobic metabolism or mitochondrial respiration. We also revealed that elevated ROS levels were the result of accumulation rather than increased production, i.e. the high levels of ROS induced by Arg with Leu were mainly derived from accumulation due to GPx4 reduction and GSH supply shortage. Although Arg with Leu decreased GPx4 and GSH levels, GPx4 and GSH remained in the nuclei. ROS causes DNA damage and induces apoptosis (49, 50). The antiapoptotic protein, Bcl-2, has been implicated in the maintenance of high nuclear GSH concentrations (51, 52). GPx4 has three physiological isoforms, cytosolic (cGPx4), mitochondrial (mGPx4), and nuclear (nGPx4), which are encoded by distinct 1a and 1b exons. They exhibit overlapping and distinct functions in the regulation of development and cell death (53). Therefore, the reduction of cytoplasmic GPx4 and GSH induces ROS accumulation, followed by integrin α5β1 expression, whereas nuclear GPx4 and GSH suggest a protective function against DNA damage. Our previous studies demonstrated that selective proteolysis in blastocysts via the ubiquitin-proteasome pathway is associated with blastocyst implantation completion (5, 7). Therefore, it is possible that the specific reduction in cytoplasmic GPx4, not in the nuclei, is derived from selective proteolysis.

The present study demonstrated that Arg alone decreased blastocyst implantation ability. Although integrin α5β1expression was not induced by Arg alone, O_2 consumption and ROS levels were similar to Arg with Leu. A previous study suggested that Arg and Leu activate mTORC1 and act independently and additively to induce trophoblast outgrowth, i.e. protein translation is required to promote changes in trophectoderm cell motility (14). Therefore, the failure to induce the expression of integrin α5β1 by Arg alone in blastocysts may be a result of the different mTORC1-mediated actions of Arg alone and Arg with Leu. Furthermore, Arg increased NO production in blastocysts. Excessive NO levels lead to apoptosis in embryos and have deleterious effects on embryonic development (29–31). Indeed, apoptosis was upregulated by Arg alone compared to Arg with Leu, suggesting that this was also due to the distinct effects of single

and combination treatments. Meanwhile, the present and previous studies have shown that Arg decreases O_2 consumption in blastocysts (21). NO can compete with O_2 for mitochondrial cytochrome c oxidase, resulting in reduced O_2 consumption (54–56). However, our correlation analysis indicated that the decreased O_2 consumption was independent of NO production. Therefore, Arg alone is associated with NO production and apoptosis; however, this pathway does not compete with O_2. Collectively, Arg alone did not increase integrin α5β1, but increased apoptosis, resulting in decreased viability and consequently decreased implantation ability.

Although Arg with Leu upregulated integrin α5β1, the total number of cells did not differ between the control and Arg with/without Leu. The number of cells in blastocysts suggests the developmental competence (21). Our correlation analysis indicated negative correlations between cell numbers and apoptosis, while integrin α5β1 were independent of cell numbers. These results suggest that cell count is a valid indicator of viability in blastocysts during peri-implantation periods but is not a suitable indicator of implantation ability before ET. Here, we report that ROS, GPx4, and GSH can be a novel valuation index for blastocyst implantation ability before transfer. Furthermore, it is possible that antioxidant reagents, such as Vitamin C, have a negative effect on blastocysts with implantation competence conferred by higher levels of ROS and integrin α5β1, with lower levels of GPx4 and GSH.

Successful embryo implantation depends on cellular and molecular crosstalk between the uterus and embryo. Therefore, implantation rates were examined in the same recipient to determine the implantation potential of the transferred blastocysts, i.e. six untreated blastocysts (control) and six treated blastocysts were transferred into distinct uterine horns in each recipient. While the variation in the same group seemed slightly high because one transferred blastocyst was 16.7% (six blastocysts were transferred into each uterine horn), the present study demonstrated that the combination of Arg and Leu exerted effects on IVF-derived mouse blastocysts. Although elevated ROS levels induced by Arg with Leu stimulated integrin α5β1 expression followed by enhanced implantation capacity in blastocysts, the levels of ROS and integrin α5β1 were dispersed. Therefore, if it is possible to select blastocysts with highly elevated ROS levels induced by Arg with Leu, the successful outcome of ART may be improved.

Materials and methods

Animals

Experimental procedures in this study were performed in accordance with the instructions of the Guide for the Care and Use of Laboratory Animals published by Utsunomiya University. Animals were housed in a temperature-controlled environment with a 14-h light, 10-h dark lighting cycle, and free access to food and water. Adult ICR mice were purchased from Japan SLC and bred at our animal care facility.

IVF and embryo culture

IVF and embryo culture were performed as previously described (57, 58) with slight modifications. Female mice were subjected to superovulation by intraperitoneal injection of equine chorionic gonadotropin (eCG) followed by 5 IU human (h)CG 48 h later. Ovulated oocytes were collected in human tubal fluid (HTF) medium without phenol red (HTF-P), 14 h after hCG injection. Spermatozoa were pre-incubated for 2–3 h in HTF-P to allow capacitation; the final concentration was 700 spermatozoa/μL. Four hours after insemination, oocytes were cultured in 100 μL of potassium simplex optimized medium (KSOM) without phenol red (KSOM-P) overlaid with paraffin liquid (Nacalai Tesque) in a humidified atmosphere of 5% CO_2 at 37°C for 90–96 h. Blastocysts were then treated with 0.2 mM L-Arg and/or 0.2 mM L-Leu (14) in four-well culture plates (Thermo Fisher Scientific) containing 500 μL of KSOM-P for 24 h as described previously (6) with slight modifications. To examine the correlation between ROS levels and integrin α5β1 expressions, blastocysts were treated with 40 μg/mL L-ascorbic acid, as described previously (59, 60).

Embryo transfer

Embryo transfer was performed as previously described (5, 6). Six 24-h cultured blastocysts with Arg and/or Leu were transferred with HEPES-buffered KSOM-P into the uteri of recipient mice on the morning of day 4 (900–1,000 h) of pseudopregnancy (vaginal plug formation was counted as day 1), and the number of implantation sites was recorded using the blue dye method on day 6 (5, 6).

Immunohistochemical analysis

Immunohistochemistry was performed as previously described (6, 18). Embryos were fixed in 3.7% formaldehyde in Ca^{2+}- and Mg^{2+}-free Dulbecco's phosphate-buffered saline (D-PBS) at room temperature for 30 min, permeabilized in 0.25% Tween-20 in D-PBS for 5 min, and incubated overnight at 4°C with primary antibodies specific for integrin α5β1 (Merck), GPx1, and GPx4 (both from Proteintech Group). After several washes, the embryos were incubated with secondary antibodies labeled with fluorescein isothiocyanate (FITC) (MP Biomedicals) or Alexa Fluor 594 (Thermo Fisher Scientific) to visualize specific antigens. Nuclei were labeled with 5 μg/mL Hoechst 33342 (bisBenzimide H33342 trihydrochloride, Thermo Fisher Scientific) for 30 min at room temperature.

Imaging of embryos

The embryos were mounted on a glass-bottom dish (Matsunami Glass) and viewed using a TCS SP8 confocal scanning laser microscope (Leica). Fluorescence intensities were quantified using Leica Application Suite X.

NO production measurement

Embryos were incubated for 20 min with 10 μM diaminofluorescein-FM diacetate (DAF-FM DA) (Goryo Chemical) in HEPES-buffered KSOM-P supplemented with polyvinyl alcohol (PVA) instead of bovine serum albumin (BSA) (HKP). After several washes with HKP, embryos were mounted on a glass-bottom dish and measured 30 min later. DAF-FM DA was excited at 500 nm and imaged at 550 nm.

O_2 consumption measurement

The oxygen consumption of the embryos was determined using an Intracellular Oxygen Concentration Assay (Abcam) according to the manufacturer's instructions. Zona pellucidae were removed using acid Tyrode's solution, and embryos were incubated with an intracellular O_2 probe in HKP for 18 h. After several washes with HKP, embryos were mounted on a glass-bottom dish and measured 30 min later. The intracellular O_2 probe was excited at 405 nm and imaged at 630–670 nm.

Measurement of mitochondrial membrane potential ($\Delta\Psi_m$)

Embryos were incubated with 1 μM JC-1 (Cayman Chemical) in the HKP medium for 20 min. After several washes with HKP, embryos were mounted on a glass-bottom dish and measured 30 min later. Membrane potential was calculated as the ratio of red fluorescence, which reflects high mitochondrial membrane potential (J-aggregates), to green fluorescence, which reflects low mitochondrial membrane potential (J-monomers). The J-aggregates were excited at 561 nm and imaged at 560–610 nm, while the J-monomers were excited at 488 nm and imaged at 500–550 nm.

Measurement of ROS

The ROS levels of the embryos were determined using CellROX Orange Reagent (Thermo Fisher Scientific) according to the manufacturer's instructions. Embryos were incubated with 5 μM ROS detection reagent in the HKP medium for 20 min. After several washes with HKP, embryos were mounted on a glass-bottom dish and measured 30 min later. ROS detection reagent was excited at 545 nm and imaged at 565 nm.

Detection of active caspases

The active caspases in the embryos were determined using a CaspGLOW Red Active Caspase Staining Kit (BioVision) according to the manufacturer's instructions. Embryos were incubated with the detection reagent in the HKP medium for 20 min. After several washes with HKP, embryos were mounted on a glass-bottom dish and measured 30 min later. Active caspases were excited at 540 nm and imaged at 570 nm.

Measurement of GSH

The GSH levels of the embryos were determined using ThiolTracker Violet (Thermo Fisher Scientific) according to the manufacturer's instructions. Embryos were incubated with 20 μM glutathione detection reagent in the HKP medium for 20 min. After several washes with HKP and 30 min later, embryos were fixed in 3.7% formaldehyde in D-PBS. Glutathione detection reagent was excited at 405 nm and imaged at 525 nm.

Statistical analysis

Statistical analyses were performed using JMP version 13.0 (SAS Institute). Student's t test was used to evaluate differences in implantation rates. The Steel–Dwass test was used for multiple comparisons to evaluate differences in integrin $\alpha5\beta1$, O_2 consumption, NO production, $\Delta\Psi_m$, ROS levels, GPx1, GPx4, GSH, percentage of caspase-positive cells, and number of cells. Data are presented as the mean ± SEM. Correlations were determined using the Pearson correlation coefficient and linear regression analysis. Fisher's exact probability test was used to evaluate the percentage of blastocysts with both high ROS and integrin $\alpha5\beta1$ levels and with both low GPx4 and GSH levels.

Acknowledgments

We thank Masato Akaiwa, Yuko Ishida, Minami Sekiguchi, Akihiro Oya, Takumi Yazawa, and Tamon Fukaya for their technical support.

Supplementary Material

Supplementary material is available at *PNAS Nexus* online.

Funding

This work was supported in part by Japan Society for the Promotion of Science (JSPS) KAKENHI Grant Nos. 25450390, 18K05936, and 21K05903 to H.M.

Author Contributions

E.F. and H.M. designed research; M.N., M.M., D.O., E.T., M.S., and M.T. performed research; M.N., M.M., D.O., E.T., M.S., M.T., and H.M. analyzed data; and M.N., M.M., D.O., E.T., M.S., M.T., and H.M. wrote the paper.

References

1 Wyns C, *et al.* 2022. ART in Europe, 2018: results generated from European registries by ESHRE. *Hum Reprod Open*. 2022:hoac022.
2 Sunderam S, *et al.* 2022. Assisted reproductive technology surveillance—United States, 2018. *MMWR Surveill Summ*. 71:1–19.
3 Katagiri Y, *et al.* 2023. Assisted reproductive technology in Japan: a summary report for 2020 by the ethics committee of the Japan Society of Obstetrics and Gynecology. *Reprod Med Biol*. 22:e12494.
4 Zegers-Hochschild F, *et al.* 2023. ART in Latin America: the Latin American registry, 2020. *Reprod Biomed Online*. 47:103195.
5 Saito K, *et al.* 2014. Degradation of estrogen receptor alpha in activated blastocysts is associated with implantation in the delayed implantation mouse model. *Mol Hum Reprod*. 20: 384–391.
6 Takeuchi M, *et al.* 2017. Improvement of implantation potential in mouse blastocysts derived from IVF by combined treatment with prolactin, epidermal growth factor and 4-hydroxyestradiol. *Mol Hum Reprod*. 23:557–570.
7 Matsumoto H. 2017. Molecular and cellular events during blastocyst implantation in the receptive uterus: clues from mouse models. *J Reprod Dev*. 63:445–454.
8 Matsumoto H, Fukui E, Yoshizawa M. 2016. Molecular and cellular events involved in the completion of blastocyst implantation. *Reprod Med Biol*. 15:53–58.
9 Dey SK, *et al.* 2004. Molecular cues to implantation. *Endocr Rev*. 25: 341–373.
10 Wang H, Dey SK. 2006. Roadmap to embryo implantation: clues from mouse models. *Nat Rev Genet*. 7:185–199.
11 Cha J, Sun X, Dey SK. 2012. Mechanisms of implantation: strategies for successful pregnancy. *Nat Med*. 18:1754–1767.
12 Armant DR, Kaplan HA, Lennarz WJ. 1986. Fibronectin and laminin promote in vitro attachment and outgrowth of mouse blastocysts. *Dev Biol*. 116:519–523.
13 Wang J, Paria BC, Dey SK, Armant DR. 1999. Stage-specific excitation of cannabinoid receptor exhibits differential effects on mouse embryonic development. *Biol Reprod*. 60:839–844.
14 Gonzalez IM, *et al.* 2012. Leucine and arginine regulate trophoblast motility through mTOR-dependent and independent pathways in the preimplantation mouse embryo. *Dev Biol*. 361:286–300.
15 Herring CM, Bazer FW, Johnson GA, Wu G. 2018. Impacts of maternal dietary protein intake on fetal survival, growth, and development. *Exp Biol Med (Maywood)*. 243:525–533.
16 Wu G, Morris SM Jr. 1998. Arginine metabolism: nitric oxide and beyond. *Biochem J*. 336:1–17.
17 Stuehr DJ. 1999. Mammalian nitric oxide synthases. *Biochim Biophys Acta*. 1411:217–230.
18 Seki M, Takeuchi E, Fukui E, Matsumoto H. 2023. Upregulation of iNOS and phosphorylated eNOS in the implantation-induced blastocysts of mice. *Reprod Med Biol*. 22:e12545.

19 Armant DR. 2005. Blastocysts don't go it alone. Extrinsic signals fine-tune the intrinsic developmental program of trophoblast cells. *Dev Biol*. 280:260–280.

20 Fritz R, Jain C, Armant DR. 2014. Cell signaling in trophoblast-uterine communication. *Int J Dev Biol*. 58:261–271.

21 Manser RC, Leese HJ, Houghton FD. 2004. Effect of inhibiting nitric oxide production on mouse preimplantation embryo development and metabolism. *Biol Reprod*. 71:528–533.

22 Leese HJ. 2012. Metabolism of the preimplantation embryo: 40 years on. *Reproduction*. 143:417–427.

23 Van Blerkom J. 2011. Mitochondrial function in the human oocyte and embryo and their role in developmental competence. *Mitochondrion*. 11:797–813.

24 Goitre L, Pergolizzi B, Ferro E, Trabalzini L, Retta SF. 2012. Molecular crosstalk between integrins and cadherins: do reactive oxygen Species set the talk? *J Signal Transduct*. 2012:807682.

25 Sorolla MA, *et al.* 2021. Microenvironmental reactive oxygen Species in colorectal cancer: involved processes and therapeutic opportunities. *Cancers (Basel)*. 13:5037.

26 Brigelius-Flohe R, Maiorino M. 2013. Glutathione peroxidases. *Biochim Biophys Acta*. 1830:3289–3303.

27 Brigelius-Flohe R, Flohe L. 2020. Regulatory phenomena in the glutathione peroxidase superfamily. *Antioxid Redox Signal*. 33: 498–516.

28 Takahashi M. 2012. Oxidative stress and redox regulation on in vitro development of mammalian embryos. *J Reprod Dev*. 58:1–9.

29 Tranguch S, Steuerwald N, Huet-Hudson YM. 2003. Nitric oxide synthase production and nitric oxide regulation of preimplantation embryo development. *Biol Reprod*. 68:1538–1544.

30 Lee TH, *et al.* 2013. Nitric oxide modulates mitochondrial activity and apoptosis through protein S-nitrosylation for preimplantation embryo development. *J Assist Reprod Genet*. 30:1063–1072.

31 Pan X, *et al.* 2015. Nitric oxide regulates blastocyst hatching in mice. *Int J Clin Exp Med*. 8:6994–7001.

32 Ho Y, Wigglesworth K, Eppig JJ, Schultz RM. 1995. Preimplantation development of mouse embryos in KSOM: augmentation by amino acids and analysis of gene expression. *Mol Reprod Dev*. 41:232–238.

33 Lee YS, Thouas GA, Gardner DK. 2015. Developmental kinetics of cleavage stage mouse embryos are related to their subsequent carbohydrate and amino acid utilization at the blastocyst stage. *Hum Reprod*. 30:543–552.

34 Morris MB, *et al.* 2020. Selected amino acids promote mouse Pre-implantation embryo development in a growth factor-like manner. *Front Physiol*. 11:140.

35 Hirota Y. 2019. Progesterone governs endometrial proliferation-differentiation switching and blastocyst implantation. *Endocr J*. 66:199–206.

36 Ojosnegros S, Seriola A, Godeau AL, Veiga A. 2021. Embryo implantation in the laboratory: an update on current techniques. *Hum Reprod Update*. 27:501–530.

37 Yelian FD, Yang Y, Hirata JD, Schultz JF, Armant DR. 1995. Molecular interactions between fibronectin and integrins during mouse blastocyst outgrowth. *Mol Reprod Dev*. 41:435–448.

38 Schultz JF, Armant DR. 1995. Beta 1- and beta 3-class integrins mediate fibronectin binding activity at the surface of developing mouse peri-implantation blastocysts. Regulation by ligand-induced mobilization of stored receptor. *J Biol Chem*. 270:11522–11531.

39 Schultz JF, Mayernik L, Rout UK, Armant DR. 1997. Integrin trafficking regulates adhesion to fibronectin during differentiation of mouse peri-implantation blastocysts. *Dev Genet*. 21:31–43.

40 Wang J, Mayernik L, Armant DR. 2002. Integrin signaling regulates blastocyst adhesion to fibronectin at implantation: intracellular calcium transients and vesicle trafficking in primary trophoblast cells. *Dev Biol*. 245:270–279.

41 Martin PM, Sutherland AE. 2001. Exogenous amino acids regulate trophectoderm differentiation in the mouse blastocyst through an mTOR-dependent pathway. *Dev Biol*. 240:182–193.

42 Gregg D, de Carvalho DD, Kovacic H. 2004. Integrins and coagulation: a role for ROS/redox signaling? *Antioxid Redox Signal*. 6:757–764.

43 Eble JA, de Rezende FF. 2014. Redox-relevant aspects of the extracellular matrix and its cellular contacts via integrins. *Antioxid Redox Signal*. 20:1977–1993.

44 Grosche J, Meissner J, Eble JA. 2018. More than a syllable in fib-ROS-is: the role of ROS on the fibrotic extracellular matrix and on cellular contacts. *Mol Aspects Med*. 63:30–46.

45 Siauciunaite R, Foulkes NS, Calabro V, Vallone D. 2019. Evolution shapes the gene expression response to oxidative stress. *Int J Mol Sci*. 20:3040.

46 Gardiner CS, Reed DJ. 1994. Status of glutathione during oxidant-induced oxidative stress in the preimplantation mouse embryo. *Biol Reprod*. 51:1307–1314.

47 Rodriguez-Gonzalez E, Lopez-Bejar M, Mertens MJ, Paramio MT. 2003. Effects on in vitro embryo development and intracellular glutathione content of the presence of thiol compounds during maturation of prepubertal goat oocytes. *Mol Reprod Dev*. 65:446–453.

48 Covarrubias L, Hernandez-Garcia D, Schnabel D, Salas-Vidal E, Castro-Obregon S. 2008. Function of reactive oxygen species during animal development: passive or active? *Dev Biol*. 320:1–11.

49 Mailloux RJ. 2020. An update on mitochondrial reactive oxygen Species production. *Antioxidants (Basel)*. 9:472.

50 Juan CA, Perez de la Lastra JM, Plou FJ, Perez-Lebena E. 2021. The chemistry of reactive oxygen species (ROS) revisited: outlining their role in biological macromolecules (DNA, lipids and proteins) and induced pathologies. *Int J Mol Sci*. 22:4642.

51 Voehringer DW, McConkey DJ, McDonnell TJ, Brisbay S, Meyn RE. 1998. Bcl-2 expression causes redistribution of glutathione to the nucleus. *Proc Natl Acad Sci U S A*. 95:2956–2960.

52 Circu ML, Aw TY. 2008. Glutathione and apoptosis. *Free Radic Res*. 42:689–706.

53 Xie Y, Kang R, Klionsky DJ, Tang D. 2023. GPX4 in cell death, autophagy, and disease. *Autophagy*. 19:2621–2638.

54 Brown GC, Cooper CE. 1994. Nanomolar concentrations of nitric oxide reversibly inhibit synaptosomal respiration by competing with oxygen at cytochrome oxidase. *FEBS Lett*. 356:295–298.

55 Cleeter MW, Cooper JM, Darley-Usmar VM, Moncada S, Schapira AH. 1994. Reversible inhibition of cytochrome c oxidase, the terminal enzyme of the mitochondrial respiratory chain, by nitric oxide. Implications for neurodegenerative diseases. *FEBS Lett*. 345:50–54.

56 Schweizer M, Richter C. 1994. Nitric oxide potently and reversibly deenergizes mitochondria at low oxygen tension. *Biochem Biophys Res Commun*. 204:169–175.

57 Takahashi A, *et al.* 2016. Impaired female fertility in tubulointerstitial antigen-like 1-deficient mice. *J Reprod Dev*. 62:43–49.

58 Akaiwa M, Fukui E, Matsumoto H. 2020. Tubulointerstitial nephritis antigen-like 1 deficiency alleviates age-dependent depressed ovulation associated with ovarian collagen deposition in mice. *Reprod Med Biol*. 19:50–57.

59 Hu J, *et al.* 2012. Vitamin C enhances the in vitro development of porcine pre-implantation embryos by reducing oxidative stress. *Reprod Domest Anim*. 47:873–879.

60 Li Q, *et al.* 2014. Vitamin C supplementation enhances compact morulae formation but reduces the hatching blastocyst rate of bovine somatic cell nuclear transfer embryos. *Cell Reprogram*. 16:290–297.